PHOTONIC SENSORS / Vol. 6, No. 4, 2016: 351–358

A Precision Fiber Bragg Grating Interrogation System Using Long-Wavelength Vertical-Cavity Surface-Emitting Laser

Binxin HU[1*], Guangxian JIN[2], Tongyu LIU[2], and Jinyu WANG[1]

[1]*Key Laboratory of Optical Fiber Sensing Technology of Shandong Province, Laser Institute of Shandong Academy of Sciences, Jinan, 250014, China*

[2]*Shandong Micro-sensor Photonics Co. Ltd, Jinan, 250014, China*

[*]Corresponding author: Binxin HU E-mail: binxin.hu@sdlaser.cn

Abstract: This paper presents the development of a cost-effective precision fiber Bragg grating (FBG) interrogation system using long-wavelength vertical-cavity surface-emitting laser (VCSEL). Tuning properties of a long-wavelength VCSEL have been studied experimentally. An approximately quadratic dependence of its wavelength on the injection current has been observed. The overall design and key operations of this system including intensity normalization, peak detection, and quadratic curve fitting are introduced in detail. The results show that the system achieves an accuracy of 1.2 pm with a tuning range of 3 nm and a tuning rate of 1 kHz. It is demonstrated that this system is practical and effective by applied in the FBG transformer temperature monitoring.

Keywords: FBG; VCSEL; wavelength interrogation; intensity normalization; peak detection

Citation: Binxin HU, Guangxian JIN, Tongyu LIU, and Jinyu WANG, "A Precision Fiber Bragg Grating Interrogation System Using Long-Wavelength Vertical-Cavity Surface-Emitting Laser," *Photonic Sensors*, 2016, 6(4): 351–358.

1. Introduction

For some physical quantities (e.g., temperature, strain, and pressure), fiber Bragg grating (FBG) sensors yield accurate and stable measurements and offer the added benefits of electrically passive operation, immunity to electromagnetic interference, and multiplexing capabilities [1]. FBG sensors therefore have been widely used in mine safety monitoring [2], industrial automation [3], structural health monitoring [4], etc. So far, the external-cavity tunable lasers are commonly adopted in some commercial FBG interrogators (e.g., MOI SM125, NI PXIe-4844, and OSICS ECL 1560). They can deliver an accuracy of about 1 pm and larger capacity over longer fiber lengths owing to its high-optical power. However, due to their fabrication complexity, these interrogators are generally complicated and expensive [5]. This makes their usage inefficient and impractical in many field applications, such as power transformer temperature monitoring, reservoir water level monitoring, and coal face ground pressure monitoring.

In recent years, vertical-cavity surface-emitting laser (VCSEL) emitting in the 1.3-μm to 1.6-μm wavelength regime, also known as long-wavelength VCSEL, has been highly desirable for FBG sensing applications. It has some unique properties such as wide tuning range, narrow linewidth, low cost, and low power consumption [6]. Therefore, a variety of FBG interrogation solutions using VCSEL have

Received: 4 May 2016/ Revised: 31 August 2016

DOI: 10.1007/s13320-016-0339-3
Article type: Regular

been reported. Huang *et al.* implemented a fast FBG interrogation system using VCSEL [7]. Van Hoe *et al*. designed a portable integrated FBG sensing system based on a single VCSEL [8]. Mizunami *et al*. designed a power-stabilized tunable source using a VCSEL and an erbium-doped fiber amplifier (EDFA) for FBG interrogation [9]. To our knowledge, these solutions usually rely on a linear function of the injection current for the VCSEL wavelength and may be susceptible to laser noise and ultimately lead to a worse throughput in many field applications.

In this paper, the tuning properties of a long-wavelength VCSEL are studied experimentally. The wavelength versus injection current tuning curves is found approximated with a second-order polynomial. Then, the overall design and key techniques of this system including intensity normalization, peak detection, and quadratic curve fitting, are introduced in detail. In particular, the combination of a four-point peak detection method and the real-time calibration using the absorption lines of C_2H_2 realizes a uniform and predicable wavelength calculation. The results show that the system achieves an accuracy of 1.2 pm with a tuning range of 3 nm and a tuning rate of 1 kHz. Finally, it is demonstrated that this system is practical and effective when applied in the FBG transformer temperature monitoring.

2. Methodology

2.1 Tuning properties

We studied the output parameters of a long-wavelength VCSEL module (VERTILAS GmbH, Germany) operating near 1530 nm integrated with a thermoelectric cooler (TEC) and a thermistor. The experimental setup included a Keithley 2420 current source, a Keithley 2510 TEC controller, and an Agilent 86120c multi-wavelength meter. All experiments were performed at room temperature. Figure 1 shows the test results.

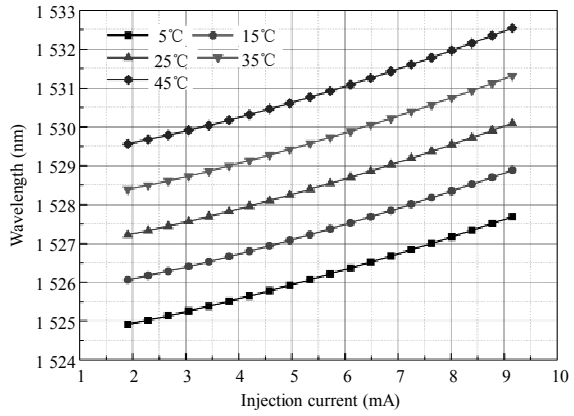

(a)

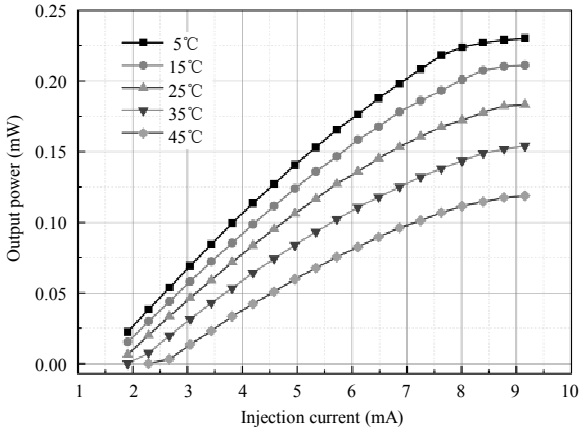

(b)

Fig. 1 Tuning curves of VCSEL module: (a) output wavelength and (b) output power vs. injection current at different heat sink temperatures.

It is evident from Fig. 1(a) that there is an approximation of wavelength tuning curves of the VCSEL by a second-order polynomial with respect to an intercept wavelength λ_0 to which a laser is tuned at the injection current and heat sink temperature T:

$$\lambda(I,T)=a(I-I_0)^2+b(I-I_0)+kT+\lambda_0 \quad (1)$$

where a, b, and k are unknown coefficients. Given that T = 25 ℃, I_0 = 1.907 mA, coefficients a, b, and k are calculated as 0.01462 nm/mA^2, 0.29146 nm/mA, and 0.11629 nm/℃, respectively. Since the coefficient k does not depend on the injection current and heat sink temperature, the wavelength of VCSELs can be tuned by the injection current and heat sink temperature

independently.

For FBG sensing purposes, an appropriate package with a temperature-controlled heat sink is used to fix the wavelength range by stabilizing the laser temperature. Wavelength tuning across the reflection spectrum of the FBG sensor is then usually realized by current tuning. For VCSELs, this mechanism works up to tuning rates even in the ~100 kHz regime [10]. Moreover, as one can see from Fig. 1(b), the output power of the VCSEL is related to both heat sink temperature and injection current. As the current decreases, so does its output power. To get precise wavelength information, variations in the light intensity of the VCSEL should be corrected by intensity normalization.

2.2 Overall design

Based on the above ideas, we designed a precise FBG sensor interrogation system, as Fig. 2 clearly shows.

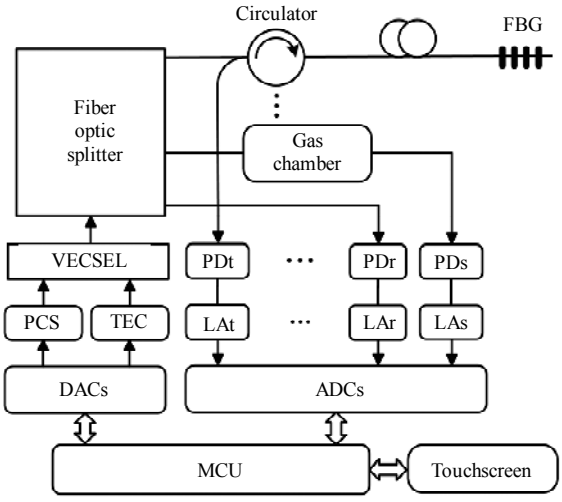

Fig. 2 Block diagram of the FBG sensor interrogation system.

The heat sink temperature of the VCSEL is maintained at a constant value (e.g., 25 ℃) by a TEC controller. A programmable current source (PCS) provides a saw-tooth modulation current (2 mA to 10 mA) with a tuning rate up to 1 kHz for the laser. The tuning signal enters a 1×16 fiber optic splitter splitting the optical signal power evenly into all the output ports. The first light is converted to a reference current by photodiode r (PDr). The second light passes through a gas chamber full of C_2H_2 and is converted to a standard current by PDs. The third light enters a circulator and reaches the sensor. The reflected light is converted to a test current by PDt. These currents are converted to the corresponding voltages by respective logarithmic amplifiers (LAs) and enter analog-to-digital converters (ADCs). The acquired data are processed by a microcontroller (MCU) to perform such operations as smoothing, normalization, peak detection, fitting, wavelength calculation, and user interface. The wavelength of the sensor is eventually displayed on a touchscreen, or sent to personal computer (PC) for further processing via an Ethernet port.

The MAX1978 serves as the TEC controller. On chip thermal control-loop circuitry can maintain a temperature stability of 0.001 ℃. The PCS is based on the AD8276 difference amplifier and the AD8603 op amp. It can drive output currents of 15 mA without the need for the external transistor or metal oxide semiconductor field effect transistor. The AD5663R, dual 16-bit digital to analog converters (DACs) are used to generate programmable reference voltages for the PCS and the TEC controller. The STM32F429 with ARM Cortex-M4 core is chosen as the MCU. The 180-MHz central processing unit (CPU), the digital signal processor (DSP) instructions, and the floating point unit make it ideal for the measurement and control applications. This device also incorporates rich peripherals such as serial peripheral interface (SPI), universal serial bus (USB), and Ethernet. The LTC1867 are used for data acquisition (DAQ), which are 16-bit, 8-channel, 200 kSPS ADCs. Two LTC1867s together form 16 channels. The MCU is linked with ADCs and DACs via the high-speed SPI interface.

2.3 Key operations

In practice, the reflected light from the FBG sensor often experiences a large amount of losses

due to connectors, splices, and fiber attenuations. The PD current is only a few nA. Meanwhile, the PD current can be hundreds of μA when local measurements are taken. The conventional gain control solutions using digital potentiometers require regulation for many times and sometimes fail. Alternatively, the LA (i.e., AD8305) can convert the PD current to a voltage with a precise logarithmic relationship and provides a large dynamic range up to 100 dB, thus more adaptive in field applications [11].

Figure 3 shows the standard signal V_s, the reference signal V_r, and the normalized signal V_n. It can be seen that there is an overestimation of time stamp for peak power of V_s due to the effect of variable light intensity.

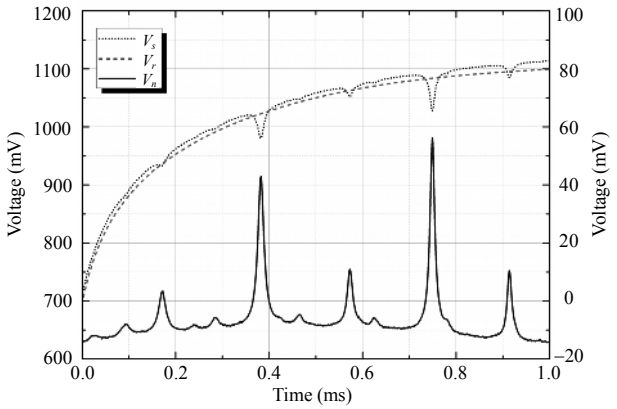

Fig. 3 Spectrums of standard, reference, and normalized signals.

Using the logarithmic transfer function of the LA, the normalized signal V_n can be expressed as

$$V_n = V_s - V_r = 0.2\log_{10}\frac{I_s}{I_r} \tag{2}$$

where I_s and I_r denote the PD currents from standard and reference channels, respectively. This normalization scheme corrects the unknown variations in the signal amplitude that accounts for the majority of random fluctuations in the average signal due to laser noise resulting in a robust sensor applicable in harsh environments.

Peak detection is another challenge for FBG sensor interrogation. The algorithm of direct peak-detection is relatively simple. But it will lead to large errors when the noise is high. Some curve fitting techniques (e.g., Gauss curve fitting, Gauss formula nonlinear curve fitting, and artificial neural network) can effectively improve the detection accuracy [12, 13]. But they are generally complicated and are not suitable for micro-controller systems. Therefore, we propose a simple and effective four-point peak detection method that can be described as:

(1) Calculate the half maximum value (V_{hm}) of the FBG reflection spectra in the specified bounds.

(2) Find two points whose ordinate is closest to V_{hm} at the left [(X_1, V_1), (X_2, V_2)] and right slopes [(X_1', V_1'), (X_2', V_2')] of the spectra.

(3) Use the line extrapolation method to get $X_1(V_{\text{hm}})$ and $X_2(V_{\text{hm}})$:

$$X(V_{\text{hm}}) = X_{k-1} + \frac{V_{\text{hm}} - V_{k-1}}{V_k - V_{k-1}},\ V_{k-1} < V_{\text{hm}} < V_k . \tag{3}$$

(4) The detection result is thus calculated as

$$X^* = \frac{X_1(V_{\text{hm}}) + X_2(V_{\text{hm}})}{2}. \tag{4}$$

Using this method, we can get five peak values of the standard signal (see Fig. 3), which are 0.16637 ms, 0.37788 ms, 0.56833 ms, 0.74442 ms, and 0.90994 ms. By referring to HITRAN database, we also get the corresponding wavelengths of the absorption lines (C_2H_2), which are 1527.44098 nm, 1528.01418 nm, 1528.59374 nm, 1529.17972 nm, and 1529.7721 nm. Using the least squares method for quadratic curve fitting, the relationship between the wavelength and tuning time is shown in Fig. 4. Eventually, we measure the peak value of the reflected signal from the FBG sensor and calculate its wavelength using the relational expression (see Fig. 4).

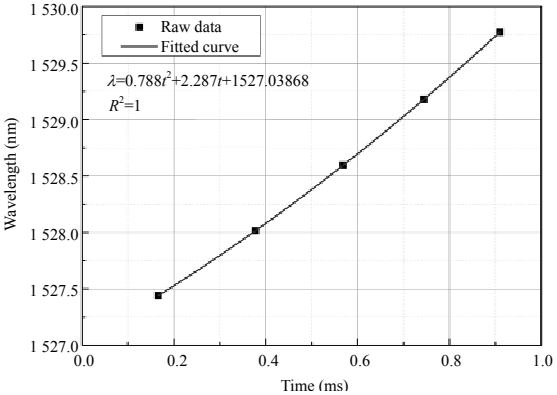

Fig. 4 Relationship between the wavelength and tuning time.

3. Results

3.1 Measurement capabilities

A photograph of the finished FBG interrogation system is shown in Fig. 5. The system is housed in a rack-mountable enclosure with dimensions of 480 mm × 87 mm × 360 mm. VCSEL, PCS, and TEC controllers are mounted on a printed circuit board (PCB), called VCSEL module. The MCU board is mounted lower right of the enclosure along with PCBs providing a touchscreen and the Ethernet interface.

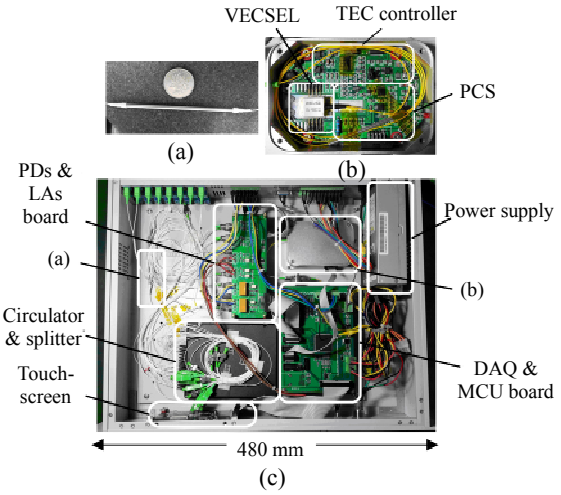

Fig. 5 Interrogation system: (a) gas chamber, (b) VCSEL module, and (c) enclosure and control electronics.

A gas chamber (C_2H_2) was used for wavelength calibration. The test conditions included the heat sink temperature of 25 ℃, current tuning rate of 1 kHz, and current running range of 2 mA to 10 mA. We repeated each measurement 100 times and used the average as the measured value. Table 1 shows the results of calibration. The accuracy is expressed as the absolute error and is found well within 1.2 pm at five standard wavelengths. In particular, the measurement uncertainties for 1528.01418 nm standard wavelength is calculated as about 1.1 pm ($k = 2$).

Another testing was to verify the spectral tuning range. The heat sink temperatures were set to 15 ℃, 25 ℃, and 35 ℃, respectively. The APEX AP204XB optical spectrum analyzer with a 0.04-pm resolution was used to measure the emitted spectrums. The test results are shown in Fig. 6.

Table 1 Results of calibration.

Standard wavelength (nm)	Measured value (nm)	Accuracy (pm)
1527.44098	1527.44039	–0.59
1528.01418	1528.01531	1.13
1528.59374	1528.59357	–0.17
1529.17972	1529.17863	–1.09
1529.7721	1529.77317	1.07

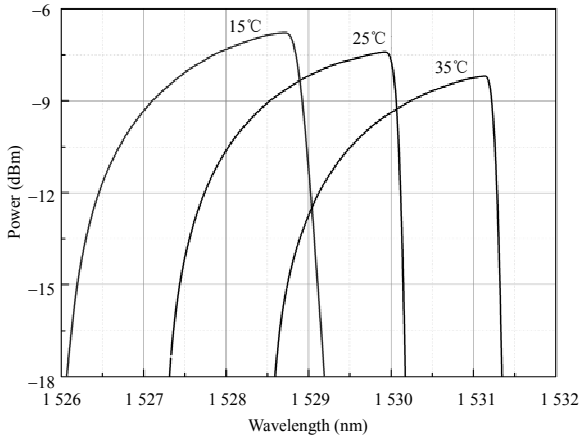

Fig. 6 Spectrum of the VCSEL output signal using current tuning (2 mA to 10 mA) at different heat sink temperatures.

It can be seen that the spectral tuning range is about 3 nm at three different temperatures and can be extended to above 5 nm when the temperature tuning is also applied. To do so, temperature tuning can be used to adjust the laser output near the central wavelength of the FBG. Moreover, this system had 14 separate optical channels. Each channel was typically connected with one FBG sensor.

3.2 Practical application

The power transformer is one of the most important devices in the power transmission and transformation system. The temperature is the main factor affecting the insulation capability [14]. The FBG sensing technology is suitable for high temperature and pressure in the oil and gas environments, thus providing a good way to the real-time monitoring of transformer temperature.

On basis of this idea, an FBG temperature sensor

(~1526.5 nm @ 25 ℃) was taken for example. And we used our interrogation system to monitor its temperature changes. The test setup included a Fluke 1502A thermometer readout together with a 5628 standard platinum resistance thermometer (0 ℃ to 300 ℃, ±0.05 ℃), a BILON CXW-501 thermostatic bath (0 ℃ to 95 ℃), and a BILON HH-05BS thermostatic bath (30 ℃ to 300 ℃).

As shown in Fig. 7, the measurement error is evaluated over a range from 0 ℃ to 230 ℃ and found well within ±0.4 ℃. This can meet high accuracy measurement requirements of transformer temperature monitoring.

The transformer had three phases (A, B, and C). Each phase included a high-voltage (HV) winding and a low-voltage (LV) winding. Besides the iron core and the camp, FBG temperature sensors were installed inside all of these windings. Our FBG interrogation system served as the temperature monitoring. The monitoring time was from 21:30 to 8:00 one day. The monitoring results are shown in Fig. 8.

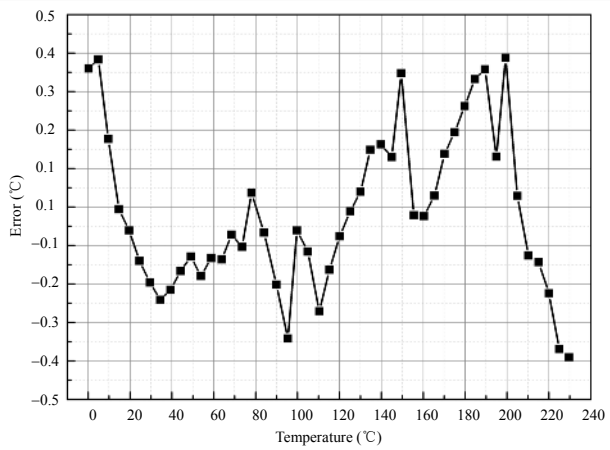

Fig. 7 FBG temperature measurements evaluation.

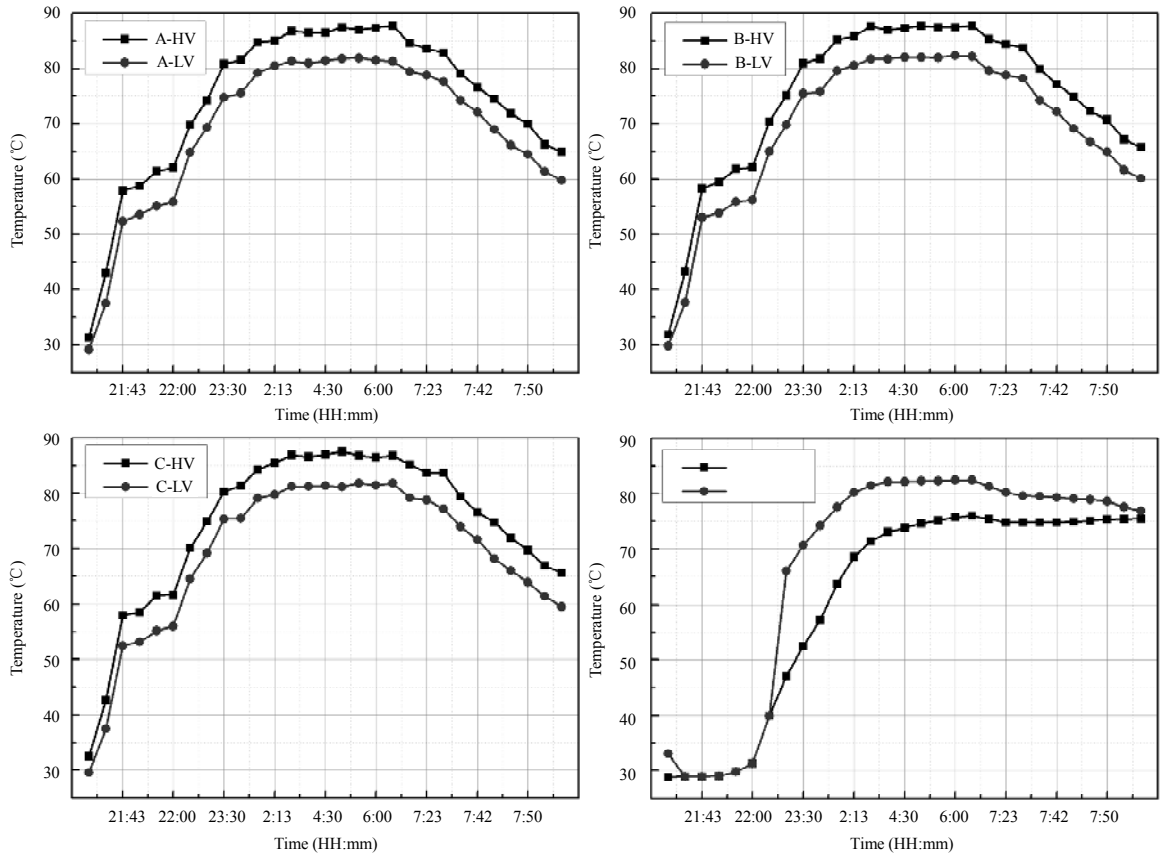

Fig. 8 FBG transformer temperature monitoring results.

It can be seen that the maximum temperature is about 90 ℃ for the HV winding of B phase. All temperatures rise along with the transformer running. As the power cut time (6:30) is approached, the temperatures of all windings gradually decrease to about 60 ℃. Meanwhile, the temperatures of the iron core and clamp are kept about 75 ℃. For an oil-immersed transformer with class-A insulation, the working temperature does not exceed to 105 ℃ [15]. Higher temperature will reduce the quality of mineral oil, thus reducing the transformer life and premature failure.

4. Conclusions

Those FBG interrogators based on external-cavity tunable laser are generally complicated and expensive, thus not suitable for many field applications. Therefore, a cost-effective precision FBG interrogation system using the long-wavelength VCSEL has been developed. The experimental study of tuning properties of a long-wavelength VCSEL indicates that there is an approximately quadratic dependence of its wavelength on the injection current. The proposal of this paper is to use a four-point peak detection method and the real-time calibration using the absorption lines of C_2H_2 to realize a uniform and predictable wavelength calculation. Owing to logarithmic amplifiers, the system has a large optical dynamic range. The results show that the system achieves an accuracy of 1.2 pm with a tuning range of 3 nm and a tuning rate of 1 kHz. It is demonstrated that this system is practical and effective by applied in the transformer temperature monitoring. Furthermore, the system can also be used to interrogate some dynamic signals such as acceleration, vibration, and shock.

Acknowledgment

This work was partly supported by the Science and Technology Development Plan of Shandong Province (Grant No. 2014GSF120017) and Science Fund for Young Scholars of Shandong Academy of Sciences (Grant No. 2013QN005).

References

[1] A. Zhang, S. Gao, G. Yan, and Y. Bai, "Advances in optical fiber Bragg grating sensor technologies," *Photonic Sensors*, 2012, 2(1): 1–13.

[2] J. Wang, T. Liu, G. Song, H. Xie, L. Li, X. Deng, *et al*., "Fiber Bragg grating (FBG) sensors used in coal mines," *Photonic Sensors*, 2014, 4(2): 120–124.

[3] J. Song, Q. Jiang, Y. Huang, Y. Li, Y. Jia, X. Rong, *et al*., "Research on pressure tactile sensing technology based on fiber Bragg grating array," *Photonic Sensors*, 2015, 5(3): 263–272.

[4] S. Ma, J. Guo, Y. Guo, J. Chao, and B. Zhang, "On-line monitoring system for downhole temperature and pressure," *Optical Engineering*, 2014, 53(8): 087102.

[5] V. R. Pachava, S. Kamineni, S. S. Madhuvarasu, K. Putha, and V. R. Mamidi, "FBG based high sensitive pressure sensor and its low-cost interrogation system with enhanced resolution," *Photonic Sensors*, 2015, 5(4): 1–9.

[6] H. Nasim and Y. Jamil, "Recent advancements in spectroscopy using tunable diode lasers," *Laser Physics Letters*, 2013, 10(4): 916–923.

[7] Y. Huang, T. Guo, C. Lu, and H. Y. Tam, "VCSEL-based tilted fiber grating vibration sensing system," *IEEE Photonics Technology Letters*, 2010, 22(1): 1235–1237.

[8] B. V. Hoe, G. Lee, E. Bosman, J. Missinne, and S. Kalathimekkad, "Ultra small integrated optical fiber sensing system," *Sensors*, 2012, 12(9): 12052–12069.

[9] T. Mizunami, S. Hirose, T. Yoshinaga, and K. I. Yamamoto, "Power-stabilized tunable narrow-band source using a VCSEL and an EDFA for FBG sensor interrogation," *Measurement Science and Technology*, 2013, 24(9): 094017–094023.

[10] A. Lytkine, W. Jäger, and J. Tulip, "Frequency tuning of long-wavelength VCSELs," *Spectrochimica Acta Part A: Molecular and Biomolecular Spectroscopy*, 2006, 63(5): 940–946.

[11] M. Fernandez-Vallejo and M. Lopez-Amo, "Optical fiber networks for remote fiber optic sensors," *Sensors*, 2012, 12(4): 3929–3951.

[12] P. Wang P, X. Han, S. Guan, H. Zhao, and M. Shao, "Research on peak-detection algorithm for high-precision demodulation system of fiber Bragg grating," *International Journal of Hybrid Information Technology*, 2014, 7(6): 337–344.

[13] M. Basu and S. K. Ghorai, "Sequential interrogation of multiple FBG sensors using LPG modulation and an artificial neural network," *Measurement Science and Technology*, 2015, 26(4):1–9.

[14] X. Zhang, R. Huang, W. Huang, S. Yao, D. Hou, and M. Zheng, "Real-time temperature monitoring system using FBG sensors on an oil-immersed power transformer," *High Voltage Engineering*, 2014, 40(2): 253–259.

[15] M. R. Meshkatoddini and S. Abbospour, "Aging study and lifetime estimation of transformer mineral oil," *American Journal of Engineering and Applied Sciences*, 2008, 1(4): 384–388.